Cell Death and Differentiation (2014) 21, 811–824

www.nature.com/cdd

MDM2 restrains estrogen-mediated AKT activation by promoting TBK1-dependent HPIP degradation

K Shostak[1,2,9], F Patrascu[1,2,9], Sl Göktuna[1,2], P Close[1,2], L Borgs[1,3], L Nguyen[1,3,4], F Olivier[1,5], A Rammal[1,2], H Brinkhaus[6], M Bentires-Alj[6], J-C Marine[7,8] and A Chariot*[,1,2,4]

Restoration of p53 tumor suppressor function through inhibition of its interaction and/or enzymatic activity of its E3 ligase, MDM2, is a promising therapeutic approach to treat cancer. However, because the MDM2 targetome extends beyond p53, MDM2 inhibition may also cause unwanted activation of oncogenic pathways. Accordingly, we identified the microtubule-associated HPIP, a positive regulator of oncogenic AKT signaling, as a novel MDM2 substrate. MDM2-dependent HPIP degradation occurs in breast cancer cells on its phosphorylation by the estrogen-activated kinase TBK1. Importantly, decreasing *Mdm2* gene dosage in mouse mammary epithelial cells potentiates estrogen-dependent AKT activation owing to HPIP stabilization. In addition, we identified HPIP as a novel p53 transcriptional target, and pharmacological inhibition of MDM2 causes p53-dependent increase in HPIP transcription and also prevents HPIP degradation by turning off TBK1 activity. Our data indicate that p53 reactivation through MDM2 inhibition may result in ectopic AKT oncogenic activity by maintaining HPIP protein levels.
Cell Death and Differentiation (2014) **21,** 811–824; doi:10.1038/cdd.2014.2; published online 31 January 2014

Restoration of p53 tumor suppressor function in cancer cells expressing wild-type (WT) p53 is a promising therapeutic approach.[1] Reactivation of p53 activity can be achieved by small molecular inhibitors that disrupt the interaction between p53 and its main E3 ligase MDM2. As a result, targeted cells undergo cell cycle arrest and apoptosis through p53 stabilization.[2] A potential drawback associated with this approach is that, besides p53, MDM2 targets other substrates for degradation.[3] In this context, accumulative evidence show that MDM2 promotes the degradation of FOXO3a, a tumor-suppressing transcription factor as well as the apoptosome activator CAS and the ubiquitin E3 ligase HUWE1.[4,5] Although it is currently unclear whether MDM2 targets positive regulators of oncogenic pathways, an exhaustive characterization of MDM2 substrates will help to anticipate undesired side effects of MDM2 inhibitors used in cancer therapy.

Oncogenic pathways include AKT-dependent signaling cascades. Indeed, AKT promotes cell proliferation, survival, migration and angiogenesis by targeting numerous substrates ranging from anti-apoptotic transcription factors to regulators of protein synthesis.[6,7] Mutations or altered expressions of various AKT-activating signaling molecules have been described in human malignancies, thereby defining AKT as a hallmark of tumor development and progression.[8,9] AKT activation by estrogens requires the microtubule-binding protein hematopoietic PBX-interaction protein (HPIP).[10] Initially identified as a corepressor of pre-B-cell leukemia homeobox protein 1 (PBX1),[11] HPIP assembles a signaling complex that connects the p85 subunit of PI3K and ERα to microtubules in order to properly activate AKT.[10] Likewise, HPIP also promotes the growth and differentiation of hematopoietic cells through AKT.[12]

Because correct regulation of AKT is of paramount importance, multiple mechanisms have evolved to terminate or limit its activation. Those mechanisms involve AKT dephosphorylation by a variety of phosphatases[13–17] or its degradation by E3 ligases.[18,19]

We describe here the identification of HPIP as a MDM2 substrate. HPIP degradation by MDM2 occurs through a p53-independent pathway and on phosphorylation by TBK1, an IKK-related kinase described as a synthetic lethal partner of KRAS and as a pro-angiogenic factor.[20–22] Mdm2 deficiency in the mouse strongly increases HPIP by promoting

[1]Interdisciplinary Cluster for Applied Genoproteomics, GIGA-Research, University of Liège, Liège, Belgium; [2]Unit of Medical Chemistry, GIGA-Signal Transduction, GIGA-R, University of Liège, Liège, Belgium; [3]Developmental Neurobiology Unit, GIGA-Neurosciences, GIGA-R, University of Liège, Liège, Belgium; [4]Walloon Excellence in Life Sciences and Biotechnology (WELBIO), Wallonia, Belgium; [5]Animal Facility, University of Liege, CHU, Sart-Tilman, Liège 4000, Belgium; [6]Mechanisms of Cancer, Friedrich Miescher Institute for Biomedical Research (FMI), Basel, Switzerland; [7]Center for Human Genetics, KU Leuven, Leuven, Belgium and [8]Center for the biology of disease, VIB, KU Leuven, Leuven, Belgium

*Corresponding author: A Chariot, Laboratory of Clinical Chemistry, GIGA-R, Tour GIGA, + 2 B34, Sart-Tilman, University of Liège, CHU, Sart-Tilman, Liège 4000, Belgium. Tel: +32 4 366 2472; Fax: +32 4 366 4534; E-mail: Alain.chariot@ulg.ac.be

[9]These authors contributed equally to this work.

Keywords: TBK1; AKT; HPIP; MDM2; estrogens

Abbreviations: CAS, Cellular apoptosis susceptibility; EGF, Epithelial growth factor; ERα, Estrogen receptor alpha; GREB1, Growth regulation by estrogen in breast cancer 1; FOXO3a, Forkhead box O3; HPIP, Microtubule-binding protein hematopoietic PBX-interaction protein; HUWE1, HECT, UBA and WWE domain-containing protein 1; IKK, I kappaB alpha kinase; MDM2, Mouse double minute 2; MEC, Mammary epithelial cell; NAP1, NAK (NF-kappaB-activating kinase)-associated protein 1; NEMO, NF-kappa B essential modulator; PBX1, Pre-B-cell leukemia homeobox protein 1; PCR, Polymerase chain reaction; PI3K, Phosphatidylinositide 3-kinase; TANK, TRAF family member associated NF-kappaB activator; TBK1, TANK-binding kinase 1; TNFα, Tumor necrosis factor alpha

Received 14.6.13; revised 18.12.13; accepted 23.12.13; Edited by K Vousden; published online 31.1.14

its p53-dependent transcription and by preventing its degradation. As a result, AKT activity is sustained in mammary epithelial cells. Pharmacological inhibition of MDM2 also increases p53-dependent HPIP transcription and prevents HPIP protein degradation by turning off TBK1 activity in breast cancer cells. Therefore, our data indicate that p53 reactivation through MDM2 inhibition may result in undesired activation of AKT signaling via HPIP upregulation.

Results

HPIP is a TBK1-interacting protein. AKT signaling contributes to resistance to targeted therapies in breast cancer.[23] Given the capacity of IKK-related kinases TBK1 and IKKε to directly phosphorylate AKT,[24–26] we aimed to identify new TBK1 substrates through interactomic studies to better understand the molecular link between TBK1 and AKT. We conducted a yeast two-hybrid screen using the C-terminal domain of TBK1 (amino acids 529–729) fused to the DNA-binding domain of the GAL4 transcription factor as bait (Figure 1a). Among 47 TBK1-interacting clones, four encoded TANK, which was previously reported as a TBK1-associated protein.[27] Two clones encoded a product lacking the first 205 amino acids of HPIP, whereas a third clone encoded the C-terminal part of HPIP (amino acids 275–731) (Figure 1a). Co-immunoprecipitation (IP) experiments confirmed the interaction between exogenously expressed epitope-tagged TBK1 and HPIP in HEK293 cells (Figure 1b; Supplementary Figures S1A and S1B, see our Supplementary Data Section). In agreement with the yeast two-hybrid data, the C-terminal domain of TBK1 was necessary for the binding to HPIP, as the TBK1ΔC30 mutant failed to co-precipitate TBK1 (Figure 1b). Interestingly, the kinase-dead version of TBK1 (TBK1 KD) strongly bound HPIP, despite a weaker expression level when compared with WT TBK1 (Figure 1b). Moreover, ectopically expressed HPIP associated with endogenous TBK1, similarly to over-expressed TANK/I-TRAF, used as a positive control (Supplementary Figure S1C). Of note, IKKε, the other IKK-related kinase, also bound HPIP, as judged by co-IP studies (Supplementary Figure S1D). We also detected the binding of endogenous HPIP with NAP1 or TANK/I-TRAF, two scaffold proteins of TBK1 (Figures 1c and d).[28,29] HPIP also bound NEMO/IKKγ, the scaffold protein of the IKK complex acting in the classical NF-κB-activating pathways[30] (Figure 1d). Finally, TBK1 and HPIP also partially colocalized, as judged by immunofluorescence analysis (Figure 1e). Together, our data identify HPIP as a protein partner of TBK1 and its scaffold proteins.

TBK1 and HPIP regulate estrogen-mediated AKT activation. To explore the functional significance of the TBK1–HPIP interaction, we searched for signaling cascades in which both proteins have a critical role. HPIP was dispensable for both NF-κB- and IRF3-activating pathways (Supplementary Figure S2). Moreover, both HPIP and TBK1 were dispensable for EGF-mediated AKT and ERK1/2 activations in MCF7 cells (Supplementary Figure S3). As estrogen-mediated AKT-activation relies on HPIP, which tethers ERα to microtubules,[10] we tested whether TBK1 is involved in this signaling cascade. 17β estradiol (E2) activated TBK1, AKT and ERK1/2 in the p53 WT breast cancer cell line MCF7 (Figure 2a). Moreover, E2-stimulated AKT activation (as judged by an anti-pan phospho-AKT antibody) was defective in HPIP-depleted cells (Figure 2b). More specifically, AKT1 and AKT3, but not AKT2, phosphorylations were decreased in HPIP-depleted MCF7 cells, thus demonstrating a role for HPIP in estrogen-dependent activation of some but not all AKT isoforms (Figure 2b). Of note, E2-mediated MEK1 and ERK1/2 activations were also impaired on HPIP deficiency in MCF7 cells (Figure 2b). Finally, steady-state levels of ERα were markedly lower on HPIP depletion (Figure 2b). Therefore, HPIP critically drives the activation of multiple kinases on stimulation of estrogens and is also necessary for the integrity of ERα. Having defined the HPIP-dependent signaling pathways, we next assessed their activation status on TBK1 deficiency. Even if activated ERK1 levels were slightly enhanced on TBK1 deficiency in unstimulated cells, E2-mediated AKT and ERK1/2 activations as well as E2-induced ERα phosphorylation were all impaired in TBK1-depleted MCF7 cells (Figure 2c). Of note, HPIP levels were higher on TBK1 depletion (Figure 2c). Finally, mRNA levels of *GREB1* (growth regulation by estrogen in breast cancer 1), an early-response gene in the estrogen receptor-regulated pathway that promotes hormone-dependent cell proliferation,[31] were severely affected on HPIP or TBK1 depletion in estrogen-treated MCF7 cells (Figure 2d). Tamoxifen is a commonly used anti-estrogen therapy for hormone receptor-positive breast cancers, but resistance to this drug occurs through multiple mechanisms, including deregulated AKT activation.[32] Given the role of HPIP in AKT activation, we explored whether HPIP promotes tamoxifen resistance in breast cancer cells. Remarkably, HPIP depletion in MCF7 cells indeed sensitized them to tamoxifen (Figure 2e). Therefore, our data identify TBK1 and HPIP as essential components of the E2-dependent, ERK1/2- and AKT1/3-activating pathway necessary for ERα signaling.

Phosphorylation of HPIP on serine 147 by TBK1 promotes GREB1 expression by estrogens. As HPIP binds TBK1, we explored whether HPIP is a TBK1 substrate. Immunoprecipitated FLAG-HPIP was phosphorylated in TBK1-overexpressing cells, similarly to FLAG-TANK, a known TBK1 substrate (Figure 3a).[27] Such phosphorylation of HPIP relies on TBK1 kinase activity, as a kinase-dead version of TBK1 failed to phosphorylate HPIP. An HPIP mutant lacking the first 60 N-terminal amino acids (HPIPΔN60) was still phosphorylated by TBK1 (Supplementary Figure S4A), whereas deletion of the first 150 amino acids abolished both interaction and phosphorylation (Supplementary Figure S4A). Therefore, TBK1 phosphorylates HPIP within a domain located downstream of the first 60 N-terminal amino acids. *In silico*, we identified putative target residue(s) as serines 43, 45, 146, 147, 148 and threonine 152. As serines 146, 147 and 148 are located within the HPIP domain targeted by TBK1 (Supplementary Figure S4A; Figure 3b), we explored whether their mutation has an impact on TBK1-mediated HPIP phosphorylation. The replacement of serine 146 with alanine (S146A) only slightly affected the binding of HPIP to

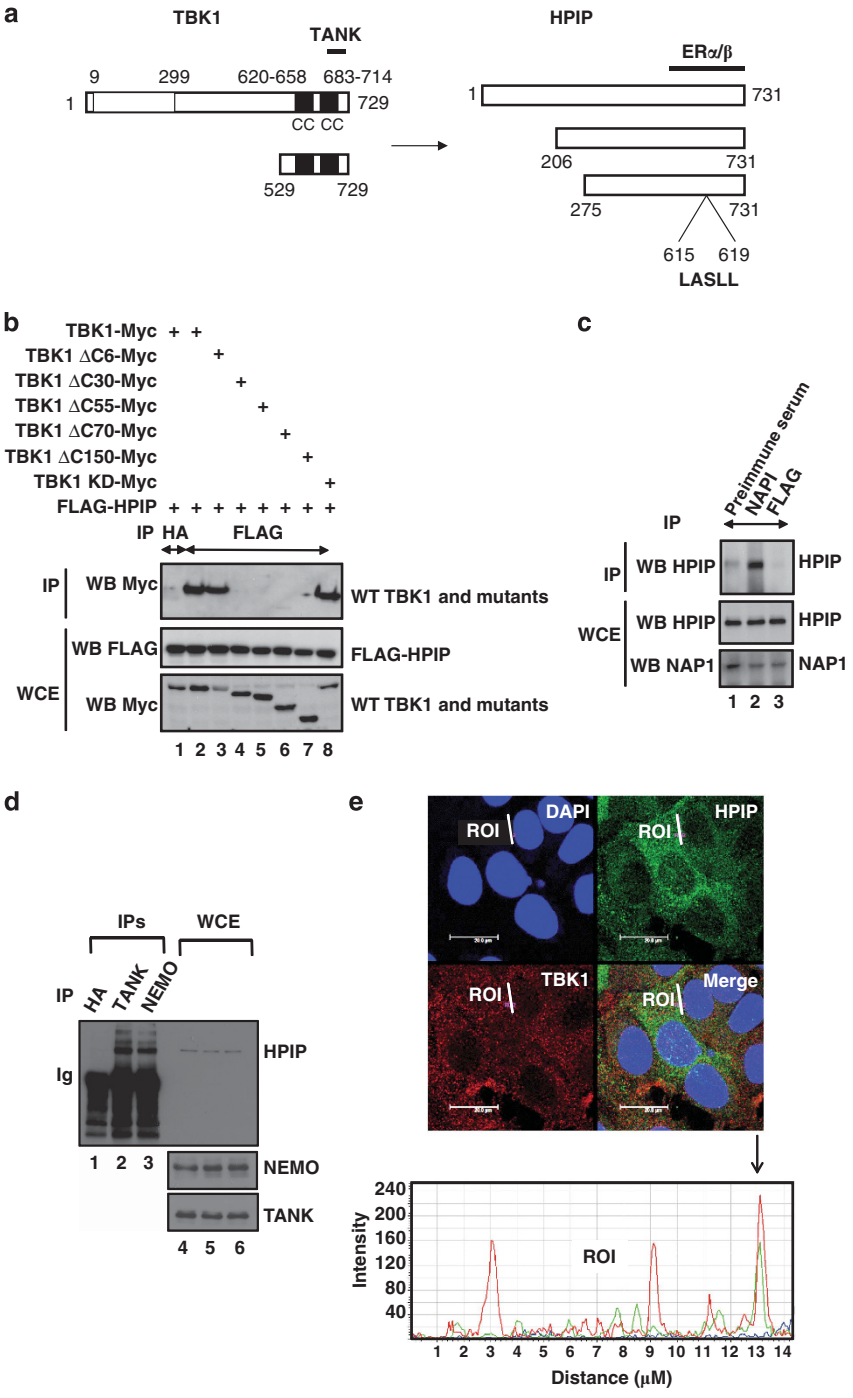

Figure 1 Identification of HPIP as a TBK1-associated protein. (**a**) Schematic representation of the bait as well as of the HPIP clones isolated from yeast two-hybrid analysis. On the left, the TBK1-coding sequence is illustrated with both the C-terminal TANK-interacting region and the coiled-coil (CC) domains. The bait includes amino acids 529–729 of TBK1 fused to the DNA-binding domain of the GAL4 transcription factor. On the right, the full HPIP cDNA sequence is depicted with both the C-terminal ERα-interacting domain as well as the LASLL sequence (LXXLL motif or nuclear receptor-interacting motif) within amino acids 615–619. (**b**) TBK1 binds HPIP through its C-terminal domain. On the left, schematic representation of the TBK1 constructs used in co-IP experiments. The N-terminal kinase domain (KD) and the coiled-coil (CC) domains are illustrated. On the right, TBK1 binds HPIP through its C-terminal region. 293 cells were transfected with the indicated expression constructs and cell extracts were subjected to anti-HA (lane 1, negative control) or -FLAG (lanes 2–8) IPs followed by an anti-Myc western blot (top panel in order to detect TBK1 or its mutants). Crude cell extracts were also used for anti-FLAG and -Myc western blots (lower panels). (**c** and **d**) NAP1, TANK and NEMO bind HPIP at the endogenous level. Extracts from ERα-positive ZR-75 breast cancer cells were subjected to anti-FLAG (**c**), -HA (**d**) (negative controls), or -NAP1 (**c**), -TANK (**d**), and -NEMO (**d**) IP followed by anti-HPIP western blots (top panels). A pre-immune serum was also used as a negative control for the experiment described in **c**. Crude cell extracts were subjected to anti-NAP1 (**c**), -NEMO (**d**), -TANK, (**d**), or -HPIP (**c** and **d**) or western blots (lower panels). (**e**) TBK1 and HPIP partially colocalize in MCF7 cells. On the top, endogenous HPIP and TBK1 were visualized by immunofluorescence. At the bottom, profiles of relative intensities of the two fluorophores along the respective white lines. ROI, region of interest

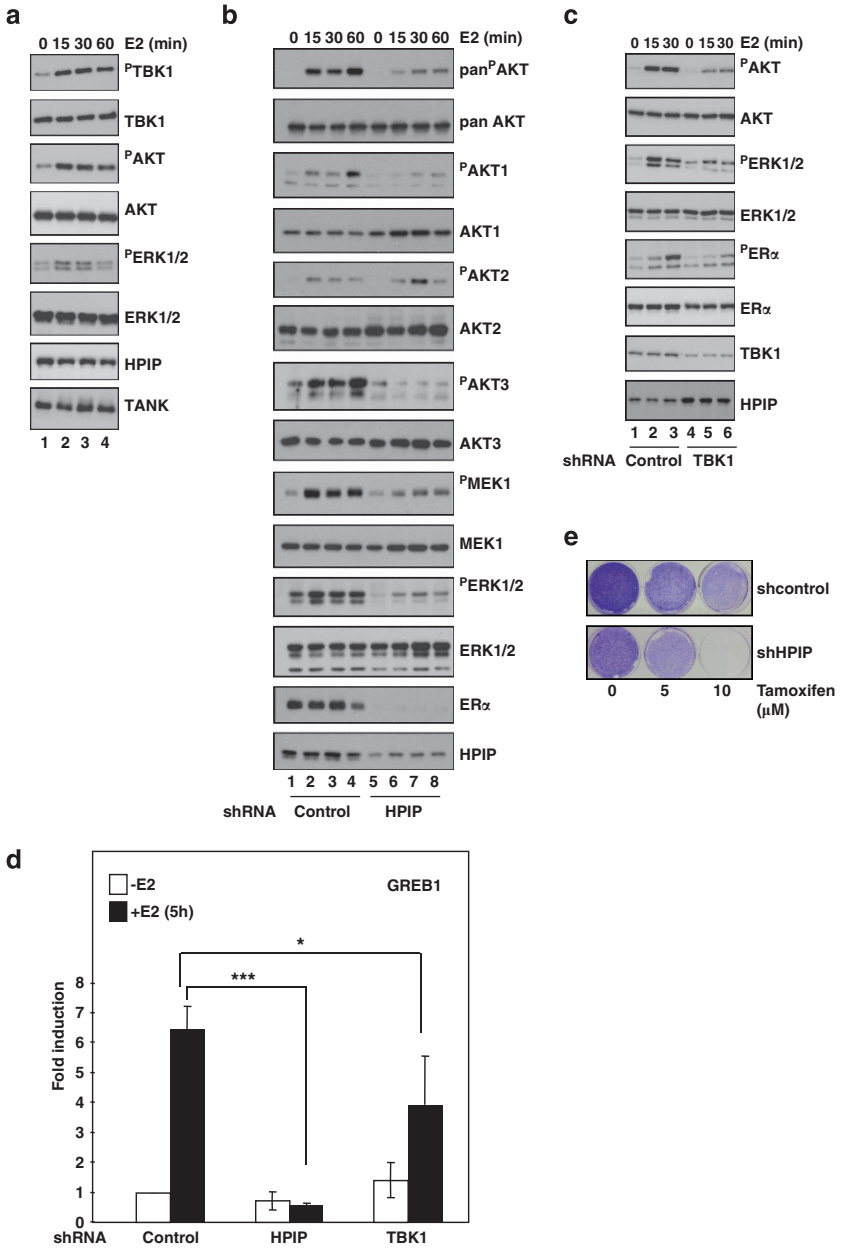

Figure 2 HPIP and TBK1 act in the estrogen-dependent and AKT-activating pathway. (**a**) E2 triggers TBK1 activation in ERα-positive breast cancer cells. MCF7 cells cultured in the appropriate medium (see Materials and Methods) were left untreated or stimulated with E2 (10 nM) for the indicated periods of time. Cell extracts were subjected to western blot (WB) analysis to assess TBK1, AKT and ERK1/2 activations. (**b** and **c**) E2-dependent AKT and ERK1/2 activations are impaired in HPIP (**b**) and TBK1 (**c**)-depleted breast cancer cells. Stably transduced shRNA control (**b** and **c**), shRNA HPIP (**b**) or shRNA TBK1 (**c**) MCF7 cells were left unstimulated or treated with E2 (10 nM) for the indicated periods of time and WB analysis using the indicated antibodies was carried out on the resulting cell extracts. (**d**) E2-mediated *GREB1* gene expression requires HPIP and TBK1. Total RNAs from control, shHPIP or shTBK1 MCF7 cells were subjected to quantitative real-time PCR analysis to assess *GREB1* mRNA levels. The abundance of *GREB1* mRNA levels in unstimulated control MCF7 cells was set to 1 and *GREB1* mRNA levels in other experimental conditions were relative to that after normalization with glyceraldehyde-3-phosphate dehydrogenase (GAPDH). The figure shows the data from three independent experiments performed on two distinct infections (mean values + S.D.) (*$P<0.05$, ***$P<0.001$, Student's *t*-test). (**e**) HPIP depletion in breast cancer cells sensitizes to tamoxifen. MCF7 cells were infected with the indicated lentiviral constructs and subsequently left untreated or stimulated with increasing concentrations of tamoxifen. Foci were visualized after coloration with Giemsa

TBK1 and HPIP phosphorylation (Figure 3b). Conversely, the mutation of serine 147 to alanine (S147A) not only impaired the binding to TBK1 but also markedly altered HPIP phosphorylation (Figure 3b). We therefore concluded that serine 147 is the key TBK1 phosphosite. Of note, IKKε, but not the kinase-dead mutant, also phosphorylated HPIP on the same serine 147 residue (Supplementary Figure S4B). We next explored whether HPIP was phosphorylated by TBK1 in E2-stimulated breast cancer cells. FLAG-HPIP was immunoprecipitated from MCF7 cells and its phosphorylated forms (pHPIP) were identified using a phospho-serine (pSer) antibody. E2 indeed enhanced HPIP phosphorylation,

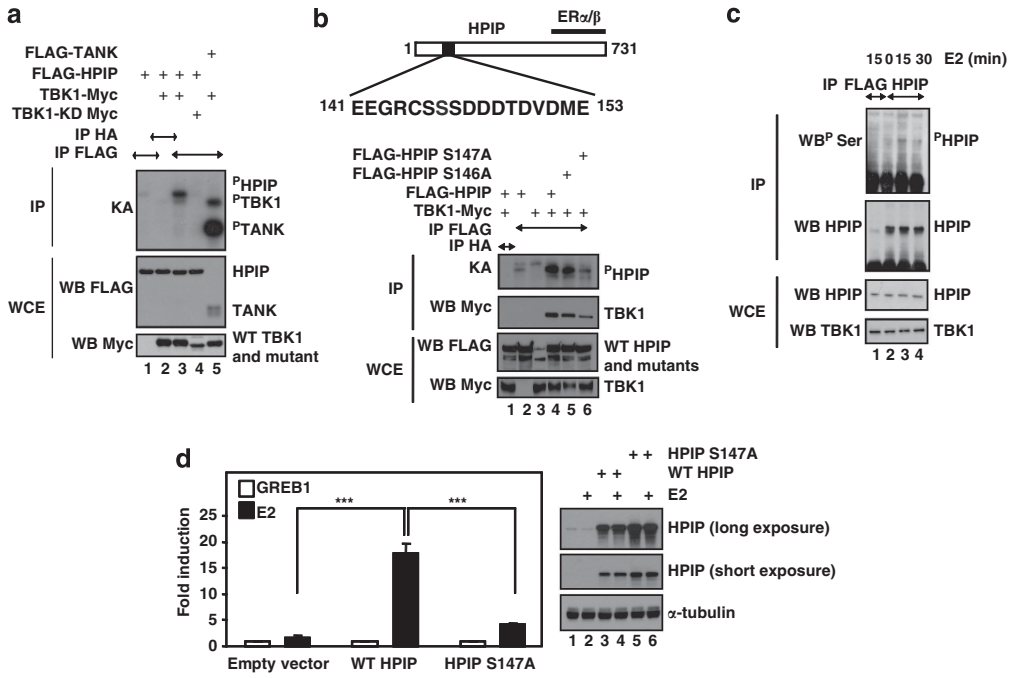

Figure 3 Phosphorylation of HPIP on serine 147 by TBK1 promotes E2-mediated GREB1 expression. (**a**) TBK1 phosphorylates HPIP. 293 cells were transfected with the indicated expression constructs and cell extracts were subjected to anti-FLAG or -HA (negative control) IPs. The resulting IPs were used as substrates for an *in vitro* kinase assay (KA) (top panels). Anti-FLAG and -Myc WBs were also performed with the crude cell extracts (lower panels). (**b**) HPIP is phosphorylated by TBK1 mainly on serine 147. The ERα/β-interacting domain on the 731 amino-acid long HPIP is depicted as well as the primary sequence from amino acids 141 to 153. 293 cells were transfected with the indicated expression constructs and cell extracts were subsequently subjected to anti-HA (negative control) or -FLAG IPs, as indicated. The resulting IPs were subjected to an *in vitro* kinase assay or an anti-Myc WB (top panel and second panel from the top). Anti-FLAG and -Myc WBs were carried out on the crude cell extracts as well (lower panels). (**c**) Endogenous HPIP is phosphorylated in an E2-dependent manner. MCF7 cells were left untreated or stimulated with E2 (10 nM) for the indicated periods of time. Cell extracts were subjected to anti-FLAG (negative control) or -HPIP IPs followed by anti-^{P}Ser or -HPIP western blots (top and second panel from the top, respectively). Cell extracts were subjected to anti-HPIP and -TBK1 WBs as well (bottom panels). (**d**) Serine 147 of HPIP is necessary to promote E2-mediated GREB1 expression. Total RNAs from untreated or E2-stimulated HPIP-depleted MCF7 cells complemented with an empty vector, a WT HPIP or the S417A mutant-expressing construct (in which shRNA-resistant silent mutations were introduced) were subjected to quantitative real-time PCR analysis to assess GREB1 mRNA levels. The abundance of GREB1 mRNA levels in unstimulated HPIP-depleted MCF7 cells was set to 1 and GREB1 mRNA levels in other experimental conditions were relative to that after normalization with GAPDH. The figure shows the data from three independent experiments performed on two distinct infections (mean values + S.D.) (***$P<0.001$, Student's *t*-test). Anti-HPIP and α-tubulin WBs are also illustrated

especially on 30 min of stimulation (Supplementary Figure S4C). HPIP phosphorylation was not observed on TNFα stimulation (Supplementary Figure S4D). Finally, endogenous HPIP phosphorylation was also induced on E2 stimulation in MCF7 cells (Figure 3c). To gain insights into the biological significance of TBK1-mediated HPIP phosphorylation, we next assessed GREB1 mRNA expression in HPIP-depleted cells complemented with WT HPIP or with the S147A mutant having shRNA-resistant silent mutations. Although the expression of WT HPIP restored GREB1 mRNA expression on E2 stimulation, the expression of the HPIP S147A mutant failed to do so (Figure 3d). Therefore, HPIP phosphorylation on serine 147 is necessary for estrogen-mediated GREB1 expression.

TBK1 promotes HPIP degradation through a phospho-dependent pathway. Given that HPIP levels are increased in TBK1-depleted and ERα-positive BT474 and MCF7 cells but not in ERα-negative SKBR3 cells (Figure 2c and Figure 4a), we hypothesized that TBK1-mediated phosphorylation may affect HPIP protein stability. Consistently, HPIP mRNA levels were not affected by TBK1 depletion (Figure 4b). Importantly, the half-life of the HPIP protein was considerably extended in TBK1-depleted MCF7 cells, whereas the half-life of BCL-3, an oncogenic protein degraded by the E3 ligase TBLR1,[33] was not (Figure 4c). Notably, the effect that was specific to TBK1 as IKKβ depletion did not modify HPIP levels in MCF7 cells (Supplementary Figure S5). To further explore the possibility that the TBK1-containing signaling complex, which includes TANK or NAP1, negatively regulates HPIP protein levels, we depleted these scaffold proteins using three distinct siRNAs. HPIP protein levels were also increased in TANK- or NAP1-depleted MCF7 cells and this effect was further enhanced on double knockdown (Supplementary Figure S6). Finally, the half-life of the HPIP S147A mutant was greatly extended when compared with WT HPIP, suggesting that HPIP phosphorylation by TBK1 negatively regulates its stability (Figure 4d).

To gain further insights into the molecular mechanisms underlying TBK1-mediated degradation of HPIP, we investigated whether changes in HPIP protein levels were correlated with differences in its polyubiquitination status. The HPIP K48-polyubiquitination (degradative), but not the K63- (non degradative) polyubiquitination, of HPIP was severely impaired on TBK1 depletion, indicating that TBK1 promotes K48-polyubiquitination of HPIP in MCF7 cells (Figure 4e).

Moreover, the S147A mutant was not subjected to the K48-linked polyubiquitination as intensively as WT HPIP (Figure 4f). E2 stimulation, which activates TBK1, decreased HPIP levels within minutes up to 72 h in MCF7 cells (Figure 4g). As a consequence, HPIP and phosphorylated TBK1 (pTBK1) levels inversely correlated on E2 stimulation (Figure 4g). Conversely, polyubiquitinated adducts on HPIP accumulated within 15 min of E2 stimulation in MG132-treated

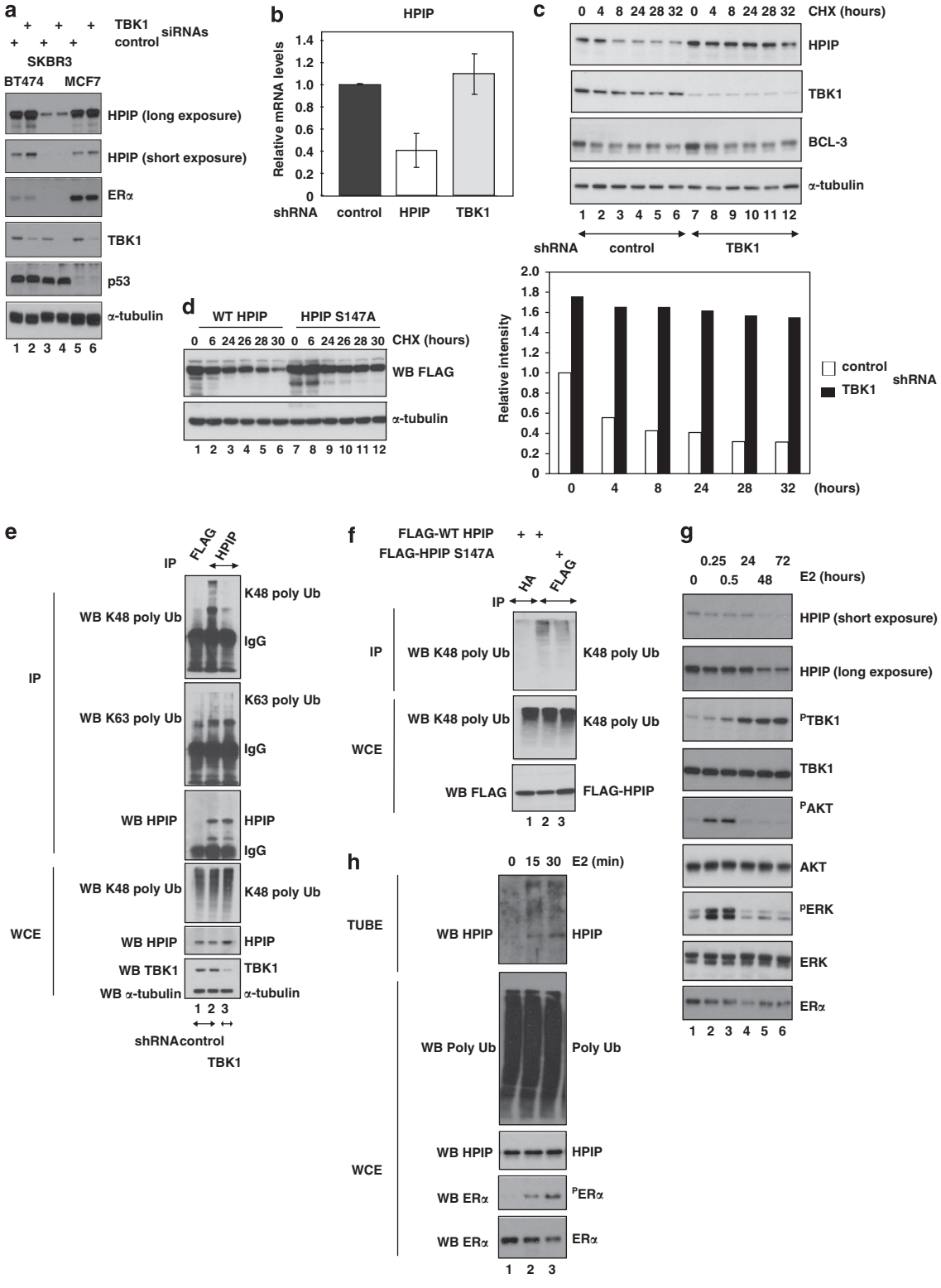

MCF7 cells and this proteasome inhibitor indeed prevented E2-mediated decrease of HPIP (Figure 4h). Taken together, these data indicate that the E2-activating TBK1-containing signaling complex negatively regulates HPIP levels by promoting its phosphorylation of serine 147, which in turn triggers its subsequent degradative polyubiquitination.

MDM2 promotes HPIP degradation through a TBK1-dependent pathway. To search for E3 ligases that promote TBK1-dependent HPIP degradation, we set up a siRNA screen in MCF7 cells using a library targeting >200 E3 ligases. Among candidates whose siRNA-mediated depletion stabilizes HPIP, MDM2 was selected for further investigation given the previously established link between MDM2 and estrogen signaling (Figure 5a).[34] We confirmed that HPIP is indeed stabilized in the parental MCF7 cells infected with five distinct MDM2 shRNA lentiviral constructs (Figure 5b). HPIP and MDM2 protein levels were also inversely correlated in p53-depleted cells, indicating that MDM2 negatively regulates HPIP levels in a p53-independent manner. Consistently, FLAG-HPIP levels were decreased in MDM2-overexpressing HEK293 cells (Supplementary Figures S7A and S7B). Interestingly, the HPIP S147A mutant that escapes TBK1-mediated phosphorylation was not destabilized (Supplementary Figures S7A and S7B). Moreover, the HPIPΔ141–153 mutant carrying a 17 amino-acid deletion that includes serines 146, 147 and 148, was also resistant to MDM2-mediated destabilization (Supplementary Figures S7A and S7B). Yet, FLAG-HPIP, HPIP S147A and HPIPΔ141–153, all efficiently bound MDM2, as evidenced by co-IP experiments in HEK293 cells (Supplementary Figure S7A). Ectopically expressed p53 (positive control) and HPIP, but not the Δ141–153 mutant, were also destabilized on MDM2 expression in MCF7 cells (Figure 5c). MDM2-mediated HPIP degradation was proteasome-dependent, as HPIP failed to be degraded by MDM2 in cells pretreated with the proteasome inhibitor MG132 (Supplementary Figure S7C). Importantly, an endogenous interaction between MDM2 and HPIP was also detected in MCF7 cells and it was not modulated by E2 (Figure 5D). To explore whether MDM2 limits HPIP protein levels by promoting its polyubiquitination, we assessed endogenous HPIP polyubiquitination in a MG132-pretreated control *versus* MDM2-overexpressing MCF7 cells. HPIP polyubiquitination was enhanced on MDM2 expression (Figure 5e). We next wondered whether HPIP polyubiquitination requires MDM2 E3 ligase activity by coexpressing p53 (positive control) or HPIP with MDM2 or with a catalytic mutant (C464A, referred to as 'Mut MDM2'). We performed co-IP experiments in denaturing conditions and detected polyubiquitination adducts on p53 and on HPIP only when coexpressed with WT MDM2 (Figure 5f). MDM2 was not found in the anti-HPIP immunoprecipitates in those denaturing conditions (Supplementary Figure S8). Therefore, HPIP, but not any HPIP-associated proteins, is subjected to MDM2-dependent polyubiquitination. To investigate whether MDM2 directly promotes HPIP polyubiquitination, we incubated a purified GST-HPIP protein with ATP, E1, E2 and recombinant human MDM2 (HDM2) *in vitro*. Polyubiquitinated adducts were detected in these experimental conditions, indicating that MDM2 directly targets HPIP for polyubiquitination (Figure 5g). Taken together, our data identify HPIP as a novel MDM2 substrate.

It has been previously demonstrated that MDM2 more efficiently targets some of its substrates for degradation once released from p53 by Nutlin, a small molecule that disrupts the MDM2–p53 complexes.[35] As expected, p53 was stabilized in MCF7 cells treated with Nutlin (Figure 6a). Although a slight increase in HPIP levels was observed in control MCF7 cells on Nutlin exposure, HPIP levels were decreased in p53-depleted cells (Figure 6a). Thus, the consequence of Nutlin treatment on HPIP protein levels is strictly dependent on the p53 status in breast cancer cells. This experiment indicates that HPIP expression may be induced by p53. Accordingly, both *p21*, a well-established p53-target gene, and HPIP mRNA levels were induced in parental but not in p53-depleted cells exposed to Nutlin, indicating that HPIP expression is transcriptionally regulated by p53 (Figure 6b). Consistently,

Figure 4 TBK1 triggers HPIP degradation through a phospho-dependent mechanism. (**a**) HPIP levels increases on TBK1 depletion in ERα-positive breast cancer cell lines. HPIP, TBK1, p53 and α-tubulin protein levels were assessed by WB in control or TBK1-depleted BT474, SKBR3 or MCF7 cells. (**b**) HPIP mRNA levels are not regulated by TBK1. Total RNAs from control, shHPIP or shTBK1 MCF7 cells were subjected to quantitative real-time PCR analysis to assess HPIP mRNA levels. The abundance of HPIP mRNA levels in control MCF7 cells was set to 1 and HPIP mRNA levels in other experimental conditions were relative to that after normalization with GAPDH. The figure shows the data from three independent experiments performed on two distinct infections (mean values + S.D.). (**c**) HPIP, but not BCL-3, half-life is extended in TBK1-depleted ERα-positive breast cancer cells. On the top, stably transduced shRNA control or shRNA TBK1 MCF7 cells were left untreated or stimulated with cycloheximide (CHX) for the indicated periods of time, and WBs using the indicated antibodies were conducted on the resulting cell extracts. At the bottom, quantification of the ratio HPIP/α-tubulin protein levels in control *versus* TBK1-depleted cells. The value obtained in control and unstimulated cells was set to 1 and values in other experimental conditions were relative to that. (**d**) Extended half-life of the HPIP S147A mutant. MCF7 cells were transfected with WT FLAG-HPIP or with the S147A mutant and the resulting cells were left untreated or stimulated with CHX for the indicated periods of time. Anti-HPIP and -α-tubulin WBs were conducted on the cell extracts. (**e**) Impaired K48-linked HPIP polyubiquitination in TBK1-depleted ERα-positive breast cancer cells. Cell extracts from stably transduced shRNA control or TBK1 MCF7 cells were subjected to anti-FLAG (negative control, lane 1) or -HPIP IPs (lanes 2 and 3) followed by WBs using anti-K48- or K63-linkage-specific polyubiquitin or HPIP antibodies. Crude cell extracts were subjected to anti-K48 poly Ub, -HPIP, -TBK1 and -α-tubulin WBs as well (lower panels). (**f**) Defective K48-linked polyubiquitination of the HPIP S147A mutant. MCF7 cells were transfected with the indicated expression plasmids and anti-K48 poly Ub WBs were performed on the anti-HA (negative control) or -FLAG IPs (top panel). Cell extracts were subjected to anti-K48 poly Ub and -FLAG WBs as well (bottom panels). (**g**) Prolonged E2 stimulation decreases HPIP levels. MCF7 cells were left untreated or stimulated with E2 (10 nM) for the indicated periods of time and the resulting cell extracts were subjected to WBs. (**h**) E2 stimulation triggers polyubiquitination of HPIP in a time-dependent manner. MCF7 cells were pretreated with MG132 (20 μM) for 2 h and subsequently stimulated or not with E2 (10 nM) for the indicated periods of time. Cell extracts obtained in denaturing conditions were diluted up to 0.1% SDS and subsequently incubated with TUBE agarose beads to trap polyubiquitinated proteins (see Materials and Methods for details) and the resulting extracts were subjected to anti-HPIP WBs (top panel). Anti-^{P}ERα and -ERα western blots performed on cell extracts were also carried out to demonstrate E2-mediated ERα phosphorylation and subsequent disappearance from the cytoplasm (bottom panel). Cell extracts were also subjected to anti-HPIP and -Poly Ub western blots (bottom panels)

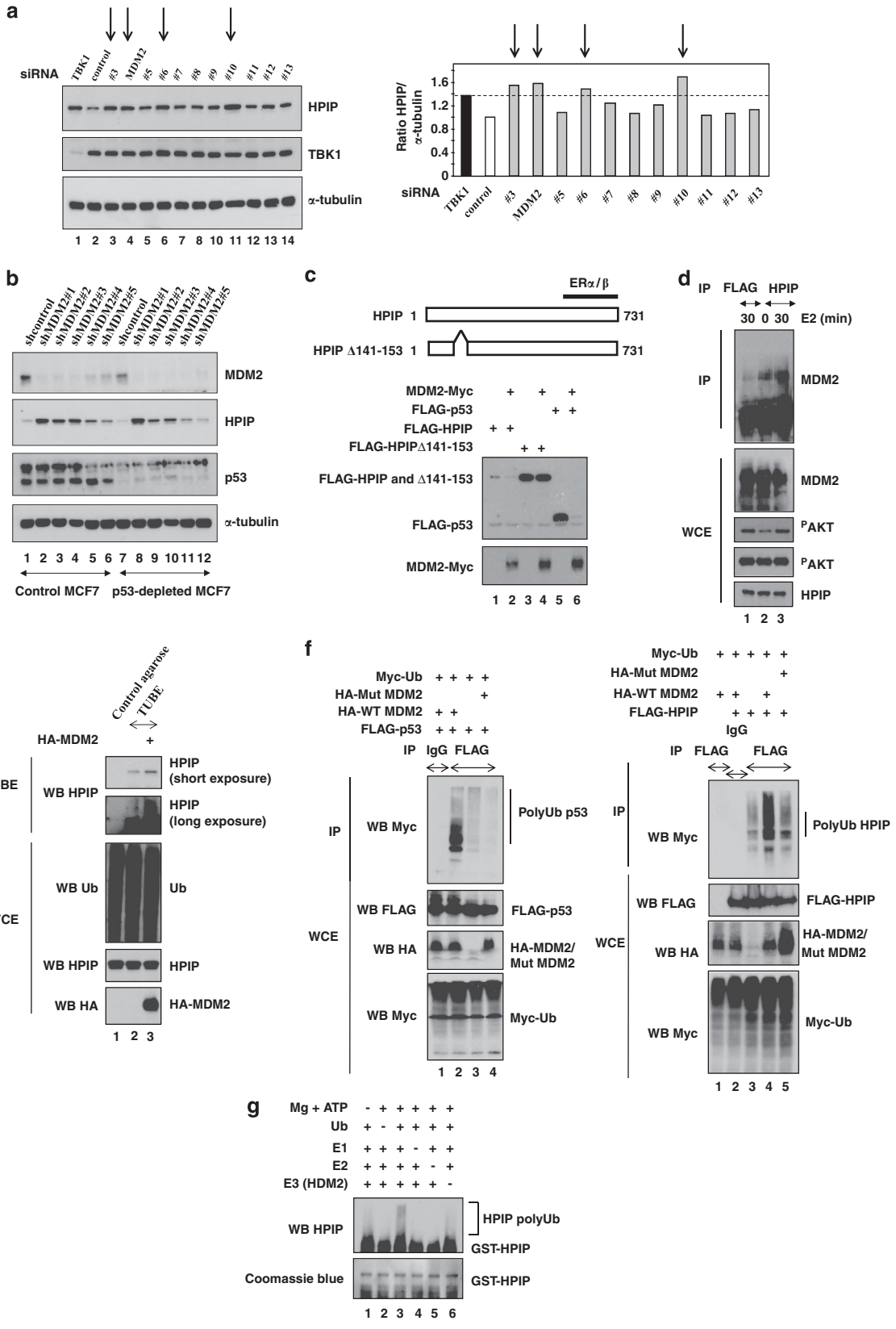
a
siRNA
TBK1
control
#3
MDM2
#5
#6
#7
#8
#9
#10
#11
#12
#13
HPIP
TBK1
α-tubulin
1 2 3 4 5 6 7 8 10 11 12 13 14
Ratio HPIP/ α-tubulin
1.6
1.2
0.8
0.4
0
b
shcontrol
shMDM2#1
shMDM2#2
shMDM2#3
shMDM2#4
shMDM2#5
MDM2
HPIP
p53
α-tubulin
1 2 3 4 5 6 7 8 9 10 11 12
Control MCF7
p53-depleted MCF7
c
ERα/β
HPIP 1 731
HPIP Δ141-153 1 731
MDM2-Myc
FLAG-p53
FLAG-HPIP
FLAG-HPIPΔ141-153
FLAG-HPIP and Δ141-153
FLAG-p53
MDM2-Myc
1 2 3 4 5 6
d
IP FLAG HPIP
30 0 30 E2 (min)
IP
MDM2
WCE
MDM2
PAKT
PAKT
HPIP
1 2 3
e
Control agarose
TUBE
HA-MDM2
TUBE
WB HPIP
HPIP (short exposure)
HPIP (long exposure)
WCE
WB Ub
Ub
WB HPIP
HPIP
WB HA
HA-MDM2
1 2 3
f
Myc-Ub
HA-Mut MDM2
HA-WT MDM2
FLAG-p53
FLAG-HPIP
IP IgG FLAG
IP
WB Myc
PolyUb p53
WB FLAG
FLAG-p53
WCE
WB HA
HA-MDM2/ Mut MDM2
WB Myc
Myc-Ub
1 2 3 4
IgG
IP FLAG FLAG
PolyUb HPIP
FLAG-HPIP
1 2 3 4 5
g
Mg + ATP
Ub
E1
E2
E3 (HDM2)
WB HPIP
HPIP polyUb
GST-HPIP
Coomassie blue
GST-HPIP
1 2 3 4 5 6

p53-binding sites were identified on the *HPIP* promoter, and ChIP assays demonstrated a specific recruitment of p53 to the site located 3500 bp upstream the transcription start site (sites E and F) in MCF7 cells (Figure 6c). Importantly, Nutlin not only restored p53 and consequently MDM2 levels but also markedly abolished E2-mediated TBK1 activation (Figure 6d). As a result, HPIP levels did not decrease on E2 stimulation but even slightly increased on Nutlin exposure, despite much higher levels of active MDM2 (Figure 6d). Therefore, TBK1 activation is necessary for MDM2-mediated HPIP degradation. The inhibition of the MDM2 E3 ligase activity by JNJ-2685416[36] significantly increased MDM2 expression in both control and p53-depleted cells with no consequence on HPIP levels, most likely because MDM2 enzymatic activity was inactivated (Figure 6e). Of note, ERα levels also decreased on JNJ-2685416 exposure (Figure 6e). Taken together, these data indicate that HPIP degradation by estrogens requires the activation of both TBK1 and MDM2. As we showed that HPIP expression is transcriptionally controlled by p53, we assessed HPIP and p53 levels in eight ER+ and six ER− breast adenocarcinomas. A strong positive correlation between both proteins was seen in all samples (Figure 6f). Taken together, our data indicate that HPIP expression is positively regulated by p53 and that MDM2 targets HPIP for degradation through a p53-independent mechanism.

MDM2 promotes E2-mediated AKT activation, limits ERα levels and contributes to tamoxifen resistance in p53-deficient breast cancer cells. Given the involvement of HPIP in ERα signaling, given the decreased ERα levels seen on restoration of MDM2 levels in Nutlin-treated MCF7 cells (see Figure 6a) and having established a direct link between MDM2 and HPIP, we next explored whether MDM2 regulated ERα levels and E2-dependent AKT activation in breast cancer cells. MDM2 deficiency in p53-depleted MCF7 cells impaired E2-mediated AKT activation, despite increased HPIP and ERα levels, as judged by western blot analysis using cytoplasmic or total protein extracts (Figures 7a and b, respectively). Therefore, MDM2 promotes E2-dependent AKT activation in p53-depleted breast cancer cells and is also involved in ERα turnover, as previously suggested.[34] Importantly, MDM2 depletion in p53-deficient MCF7 cells strongly sensitized them to tamoxifen, most likely as a result of defective AKT activation (Figure 7c). Although E2 stimulation triggered cell proliferation in p53-depleted MCF7 cells, as judged by the accumulation of cells in the S phase (from 11.1% in unstimulated cells to 23.7%), MDM2 deficiency severely impaired cell proliferation in both unstimulated and E2-treated cells (5.5% and 9.2%, respectively, see Figure 7d). Induction of GREB1 expression by estrogens was also defective in those cells (Figure 7e), thus indicating that MDM2 is necessary for estrogen signaling and cell proliferation in p53-depleted MCF7 cells.

MDM2 limits HPIP levels in mice and prevents aberrant E2-mediated AKT activation in p53-proficient cells. To investigate whether MDM2 negatively regulates HPIP protein levels *in vivo*, we assessed HPIP levels in mice expressing hypomorphic Mdm2 levels.[37] As expected, Mdm2 deficiency results in increased p53 levels *in vivo* (Figure 7f). Interestingly, although TBK1 protein levels remained unchanged, HPIP expression was markedly elevated on Mdm2 deficiency (Figure 7f), most likely because of both enhanced p53-dependent transcription and defective Mdm2-mediated degradation of HPIP. Increased HPIP levels were also observed in fat pads of Mdm2 hypomorphic males as well as other tissues such as the lung, heart, spleen and skeletal muscles (Figures 7g and h). Therefore, our data indicate that Mdm2 negatively regulates HPIP levels *in vivo*.

Having defined HPIP as a MDM2 substrate, we investigated how this pathway influences estrogen signaling. We isolated mammary epithelial cells (MECs) from control or Mdm2 hypomorphic mice and assessed E2-mediated AKT activation. HPIP levels were increased in these cells (Figure 7i). Moreover, AKT was more active on Mdm2 deficiency, suggesting that Mdm2 is necessary to limit AKT activation by estrogens in MECs. Taken together, our data indicate that HPIP degradation by Mdm2 is necessary to prevent excessive

Figure 5 MDM2 binds and limits HPIP protein levels in a TBK1-dependent manner. (**a**) Identification of MDM2 as an E3 ligase that negatively regulates HPIP protein levels. A human E3 ligase siRNA library was screened in MCF7 cells. The HPIP/α-tubulin ratio in siRNA GFP-transfected MCF7 cells (control) was set to 1 and ratios obtained in other experimental conditions were relative to that (see the histogram). Positive candidates whose siRNA-mediated depletion gives rise to a similar or higher HPIP/α-tubulin ratio than the one obtained in TBK1-depleted cells were selected. A second screening was then carried out with the selected siRNA sequences for confirmatory purposes. Representative anti-HPIP, -TBK1 and α-tubulin WBs from this second screening are shown. Arrows denote the selected candidates. The secondary screening was also done with some siRNAs that did not interfere with HPIP levels when transfected in MCF7 cells. (**b**) MDM2 destabilizes HPIP in a p53-independent manner. Control or p53-depleted MCF7 cells were infected with a control shRNA lentiviral construct (shcontrol) (lanes 1 and 7, respectively) or with constructs targeting five distinct sequences of MDM2 (shMDM2 #1 to #5) (lanes 2–6 and 8–12, respectively) and anti-MDM2, -HPIP, p53 and -α-tubulin WBs were carried out. (**c**) MDM2-mediated HPIP degradation in breast cancer cells requires the domain that includes amino acids 141–153. WT HPIP and the HPIP Δ141–153 mutant are schematically represented. MCF7 cells were transfected with the indicated expression plasmids and the resulting cell extracts were subjected to WB analysis. (**d**) MDM2 binds HPIP at the endogenous level. Untreated or E2-stimulated MCF7 cells were subjected to anti-FLAG (negative control, lane 1) or -HPIP IPs (lanes 2 and 3) followed by an anti-MDM2 WB (top panel). Crude cell extracts were subjected to anti-MDM2, -pAKT, -AKT and -HPIP WBs (bottom panels). (**e**) MDM2 promotes HPIP polyubiquitination in breast cancer-derived cells. Control (lanes 1 and 2) or MDM2-overexpressing MCF7 cells (lane 3) were treated with MG132 (20 μM) for 2 h and lysed in a NP-40-containing buffer. Cell extracts were subsequently incubated with control (lane 1) or TUBE agarose beads (lanes 2 and 3) to trap polyubiquitinated proteins and the resulting extracts were subjected to anti-HPIP WBs (top panels). Crude cell extracts were also subjected to WBs using the indicated antibodies (lower panels). (**f**) MDM2, but not a catalytic mutant, promotes p53 and HPIP polyubiquitination. 293 cells were transfected with the indicated expression plasmids, treated with MG132 (20 μM) for 2 h the next day and subsequently lysed in a denaturing lysis buffer (1% SDS). Cell extracts were subsequently diluted 10 times in order to carry out IPs using the indicated antibodies, as previously described.[44] Anti-Myc western blot analyses were performed on the resulting immunoprecipitates (top panel). Diluted cell extracts were also subjected to western blot analysis using the indicated antibodies (bottom panels). (**g**) HDM2 polyubiquitinates HPIP *in vitro*. A purified GST-HPIP protein was subjected to an *in vitro* polyubiquitination assay with a recombinant HDM2 protein. The polyubiquinated adducts of HPIP were detected by WB analysis using the anti-HPIP antibody (top panel). The purified GST-HPIP protein used as substrate was visualized on a Coomassie blue-stained gel (bottom panel)

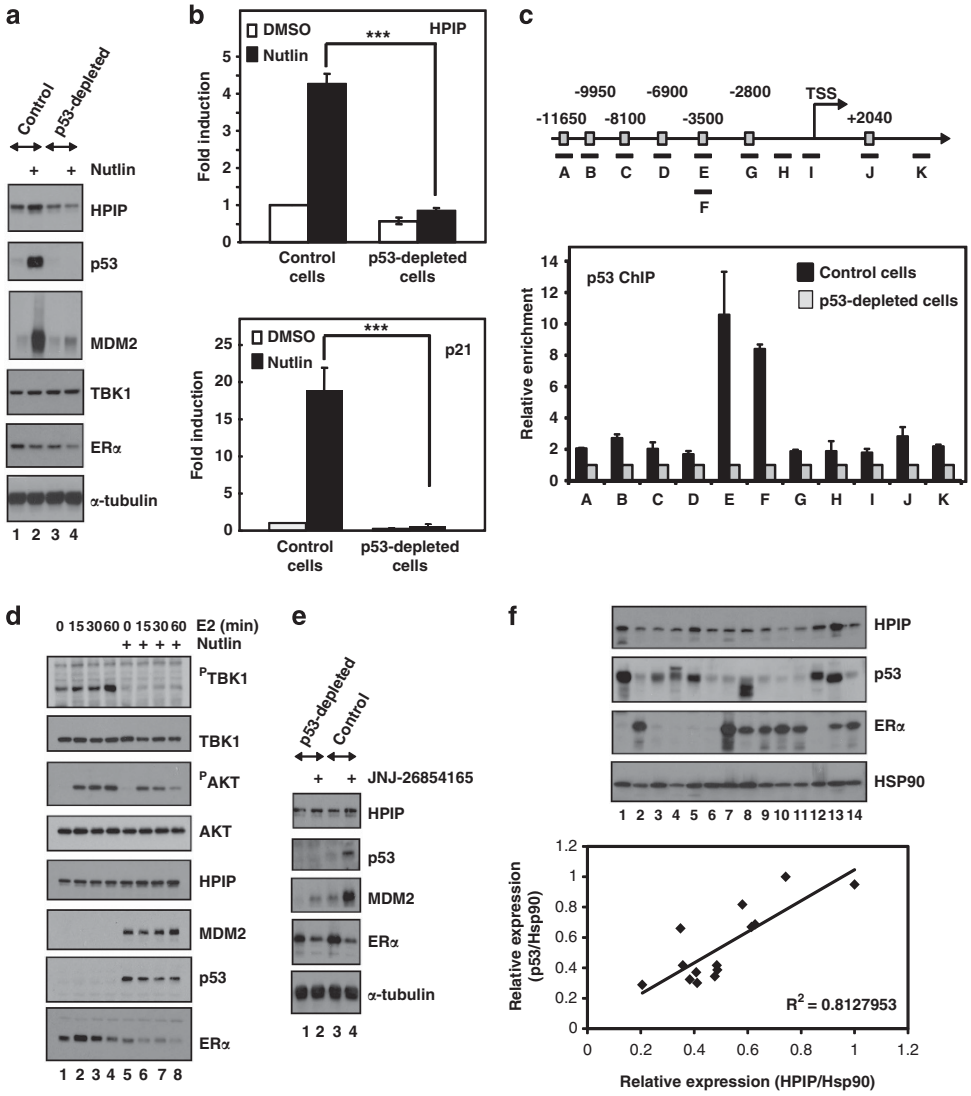

Figure 6 HPIP expression is p53-dependent. (**a**) Nutlin decreases HPIP protein levels in p53-deficient but not in WT MCF7 cells. Indicated cells were left untreated (DMSO only) or stimulated with Nutlin (10 μM) for 16 h. WBs were carried out with the resulting cell extracts, using the indicated antibodies. (**b**) Nutlin increases both HPIP and p21 mRNA levels through p53 in breast cancer-derived cells. Control or p53-depleted MCF7 cells were unstimulated (DMSO) or treated with Nutlin, and total RNAs from the resulting cells were subjected to quantitative real-time PCR analysis to assess HPIP or p21 mRNA levels. The abundance of HPIP or p21 mRNA levels in control MCF7 cells was set to 1 and mRNA levels in other experimental conditions were relative to that after normalization with GAPDH. The figure shows the data from three independent experiments (mean values + S.D.) (***$P<0.001$, Student's *t*-test). (**c**) p53 recruitment on the *HPIP* promoter, as judged by chromatin IP (ChIP) assays performed using control or p53-deficient MCF7 cells. Putative p53-binding sites (illustrated as gray boxes) were identified through *in silico* analysis (see Materials and Methods for details) and primers used for real-time PCR are depicted with black lines. Sites H, I and K were randomly chosen on the *HPIP* sequence (at -1000 bp, at the TSS, and in exon 2, respectively) and used as negative controls. Values were calculated as ratios between ChIP signals obtained with the anti-p53 (specific) and or IgG (nonspecific) antibodies. For each primer pair, the ratio obtained in p53-depleted cells was set to 1 and the one obtained with control MCF7 cells was expressed relative to it. Input DNA was always used for normalization purposes. (**d**) Nutlin interferes with E2-mediated TBK1 activation. MCF7 cells were cultured in an estrogen-free medium for 72 h and subsequently left untreated or incubated with Nutlin for 16 h. The resulting cells were then left untreated or stimulated with E2 for the indicated periods of time and WB analysis was carried out on cell extracts. (**e**) An MDM2 E3 ligase inhibitor degrades ERα but not HPIP in breast cancer cells. Control or p53-deficient MCF7 cells were left untreated or stimulated with JNJ-26854165 (10 μM) for 72 h and WB analysis using the indicated antibodies was carried out on the resulting cell extracts. (**f**) HPIP and p53 protein levels positively correlate in breast cancers. At the top, HPIP, p53, ERα and TBK1 protein levels were assessed by WB in 14 cases of human breast adenocarcinomas. An anti-HSP90 WB analysis was conducted for normalization purposes. At the bottom, the correlation curve was established based on the WB data. TSS, transcription starting site

AKT activation by estrogens in p53-proficient mammary epithelial cells.

Discussion

Reactivation of the tumor suppressor activity of p53 through the use of MDM2 antagonists is a promising approach for anticancer therapy. However, a better understanding of the MDM2 targetome is critical before the introduction of such drugs into the clinic. We identified herein the microtubule-associated protein HPIP as a new MDM2 substrate. HPIP is a positive regulator of estrogen-mediated AKT activation that promotes tamoxifen resistance in breast cancer cells and as such, is the first MDM2 substrate with oncogenic properties.

This finding is unexpected, as MDM2 is known to target multiple tumor suppressor proteins such as p53 and FOXO3A.[4] Importantly, MDM2 E3 ligase activity toward HPIP is signal-dependent as HPIP degradation occurred on TBK1 activation and subsequent HPIP phosphorylation by estrogens. To our knowledge, HPIP is the first phospho-dependent MDM2 substrate. We also identified other E3 ligase candidates that negatively regulate HPIP protein levels (data not shown), yet, it remains to be seen whether they directly bind HPIP to promote its degradative polyubiquitination and if so, through which signaling pathway they promote HPIP degradation.

Our data obtained in mice as well as in p53-proficient breast cancer cells indicate that HPIP expression is enhanced on MDM2 deficiency. As a result, estrogen-mediated AKT activation is sustained. Therefore, mammary epithelial cells may prevent excessive AKT activation by disrupting the signaling platform assembled by HPIP. Such conclusion only applies to p53-proficient cells as MDM2 is, in contrast, necessary for optimal E2-mediated AKT activation and cell proliferation in p53-deficient MCF7 cells. Therefore, *p53* does not exclusively act as a tumor suppressor gene in breast cancer, as it may also drive cell survival by promoting E2-mediated AKT activation through HPIP expression.

Pharmacological inhibitors that prevented binding of MDM2 to p53 failed to degrade HPIP, as they turned off the estrogen-dependent activation of TBK1. Although AKT activation remained unchanged in those circumstances, ERα protein levels were severely decreased. Interestingly, JNJ-26854165, which inhibits MDM2 E3 ligase activity, significantly induced both p53 and MDM2 protein levels, yet HPIP expression, which is p53-dependent, did not strongly increase. This result suggests that another E3 ligase may target HPIP for degradation in circumstances in which MDM2 E3 ligase activity is inhibited.

Our data also defined HPIP and MDM2 as new candidates that promote tamoxifen resistance in breast cancer cells. As both AKT signaling and decreased ERα levels are linked to tamoxifen resistance, our data suggest that combining MDM2 and AKT inhibitors may be more efficient to trigger tumor regression and/or limit the risk of resistance acquisition to anti-estrogenic drugs.

Our data provide more insights into mechanisms by which TBK1 activates AKT and consequently promotes E2-mediated cell proliferation. Indeed, HPIP is a critical substrate whose TBK1-mediated phosphorylation promotes GREB1 expression, an ERα target gene involved in hormone-dependent proliferation (Supplementary Figure S9). HPIP provides a signaling platform that includes MDM2, TBK1 and its scaffold protein TANK for optimal activation of AKT and the ERα-dependent signal transmission on estrogen stimulation. As a result, HPIP and MDM2 promote tamoxifen resistance as AKT-activating proteins in p53-deficient MCF7 cells. Finally, we have also shown that HPIP is necessary to maintain ERα levels in breast cancer cells and that MDM2 limits ERα levels in those cells. Although the mechanisms by which ERα is degraded on stimulation remain unclear,[38] our data suggest that MDM2 indirectly destabilizes ERα protein levels by targeting HPIP for degradation.

Materials and Methods

Cell culture, biological reagents and treatments. Human primary fibroblasts, RAW 264.7 and HEK293 cells were maintained in culture as described,[27,39,40] whereas ZR-75, MCF7 and MDA-MB-231 cells were cultured in RPMI and DMEM, respectively, and supplemented with 10% fetal calf serum and antibiotics, as were p53-deficient MCF7 cells. For E2 treatments (10 nM), control or p53-deficient MCF7 cells were first cultured for 48 h with DMEM without phenol red supplemented with Charcoal/Dextran-treated FBS (DCC) (Hyclone/Fisher, Waltham, MA, USA) followed by 24 h without serum. For EGF treatments, cells were first serum starved for 24 h.

Breast adenocarcinoma samples were provided by the BioBank (CHU, Liege, Belgium) and by the St-Louis clinic (St-Louis Cedex, France). All studies with those samples were approved by the Ethical Committee.

TANK, TBK1, NAP1 and IKKβ siRNA sequences (Eurogentec, Liege, Belgium) are available on request.

FLAG-TANK, FLAG-IKKε, TBK1-Myc, TBK1 KD-Myc, TBK1-ΔC6-, -ΔC55- and -ΔC70-Myc constructs were previously described.[27] Both TBK1-ΔC70- and -ΔC150 -Myc expression plasmids were generated by PCR using TBK1-Myc as a template. The HPIP-coding sequence was subcloned into the pCMV-XL5 expression plasmid (Origen Technologies, Rockville, MD, USA). FLAG-HPIP was generated by subcloning HPIP cDNA sequence into the pcDNA3.1 FLAG vector (Invitrogen, Carlsbad, CA, USA). FLAG-ΔN60, -ΔN150 and -ΔN160 HPIP constructs were generated by PCR, using FLAG-HPIP as the template. The HPIPΔ141–153 construct was generated by first cloning a PCR-generated fragment encompassing the region from amino acids 1 to 140 into pcDNA3.1 FLAG. A second PCR-generated fragment corresponding to amino-acid 154 to the stop codon was subsequently inserted in-frame. FLAG-HPIP S147A and S146A constructs were generated with the QuickChange Site-Directed Mutagenesis kit (Agilent Technologies, Santa Clara, CA, USA), using FLAG-HPIP as the template. For knockdown-rescue approaches in HPIP-depleted cells, silent point mutations were introduced into both WT HPIP and HPIP S147A mutant.

FLAG-p53 was generated by subcloning the p53-coding sequence into the pcDNA3.1 FLAG plasmid. The HA-MDM2 expression construct was generated by subcloning the MDM2-coding sequence into the HA-pcDNA3.1 construct. The MDM2 catalytic mutant (C464A) was purchased from Addgene (Cambridge, MA, USA) and subcloned into the HA-pcDNA3.1 construct as well.

Anti-MDM2 (SMP14, sc-965), -ERα (HC-20, sc-543), -^{P}ERα^{S167} (sc-101676), -p53 (FL-393, sc-6243), -NEMO (FL-419, sc-8330), -HSP90 (H-114, sc-7947), -HA (Y-11, sc-805), -Myc (9E10, sc-40 and A-14, sc-789), -MEK1 (H8, sc-6250), -ERK1/2 (K-23, sc-94) and -Ubiquitin (sc-8017) antibodies were from Santa Cruz Biotechnology (Santa Cruz, CA, USA), whereas anti-TBK1 (#3013), -^{P}TBK1 (#5483), -panAKT (#9272), -AKT1 (#2938), -AKT2 (#3063), -AKT3 (#3788), -^{P}pan AKT^{S473} (#4058), -^{P}AKT1^{S473} (#9018), -^{P}AKT2^{S474} (#8599), -^{P}MEK1^{S217,221} (#9154) and -^{P}ERK1/2 (#4377) antibodies were from Cell Signaling Technology (Danvers, MA, USA). The anti-NAK (TBK1) antibody used for immunofluorescence analysis was from Abcam (Cambridge, UK). The anti-^{P}AKT3^{S472} antibody was from Biorbyt (Cambridge, UK). Anti-^{P}Ser (#37430) and -Ubiquitin Lys48-specific, Apu2 (05–1307) antibodies were from Qiagen GmbH (Hilden, Germany) and Millipore, Merck KGaA (Darmstadt, Germany), respectively. The anti-α-tubulin (T6074) antibody was purchased from Sigma-Aldrich (St-Louis, MO, USA). The anti-HPIP (human) (#12102-1-AP) antibody was from Proteintech Group (Chicago, IL, USA), whereas the anti-HPIP (mouse) was generated in rabbits and directed against amino acids 465–529 and 702–721 (Phoenix Europe GmbH, Karlsruhe, Germany). The anti-NAP1 antibody was also generated in rabbits and directed against amino acids 357–392 (Phoenix Europe GmbH). The anti-p53 antibody used for ChIP assays was from Diagenode (Liege, Belgium). The anti-TANK antibody was previously described.[41]

Mouse strains and mouse mammary epithelial cell isolation. *Mdm2* hypomorphic mice were previously described.[37] Mammary glands were isolated from 8 to 10-week-old virgin control or MDM2 hypomorphic females. Mammary epithelial cell (MEC) isolation was conducted by mincing mammary glands into small pieces with razor blades in a sterile manner, followed by a digestion with collagenase/hyaluronidase (STEMCELL Technologies, Grenoble, France) for 6 h at 37 °C under shaking at 125 r.p.m. The mixture was then subjected to a spin for 5 min to get rid of cellular debris. After another spin, cells were trypsinized and centrifuged again to get rid of fibroblasts in the supernatant. The resulting pellet was washed 4–5 times with DMEM/F12 supplemented with 5% FCS and 100 U penicillin/streptomycin. Purity of MECs was confirmed through

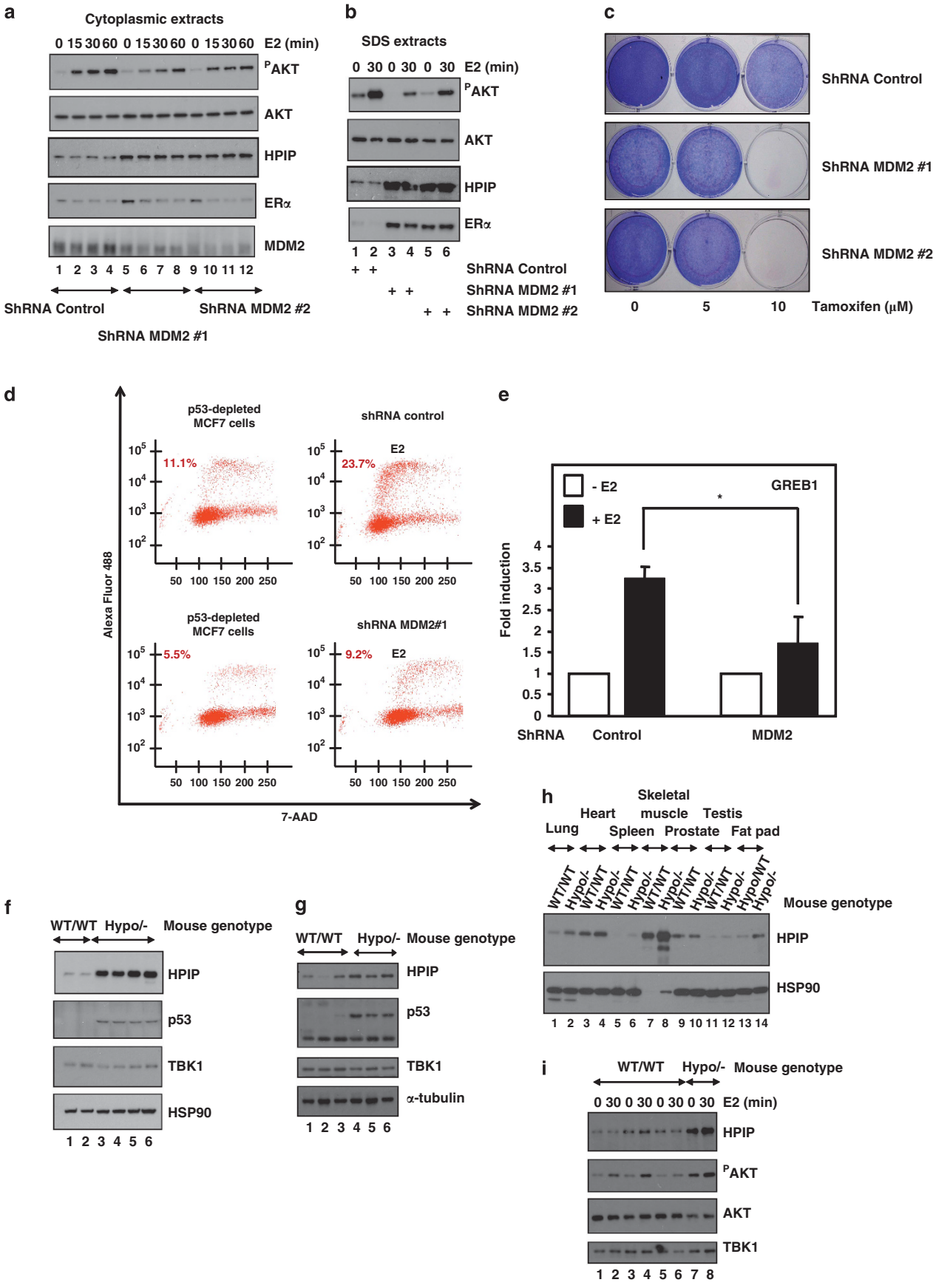
a
Cytoplasmic extracts
0 15 30 60 0 15 30 60 0 15 30 60 E2 (min)
PAKT
AKT
HPIP
ERα
MDM2
1 2 3 4 5 6 7 8 9 10 11 12
ShRNA Control
ShRNA MDM2 #2
ShRNA MDM2 #1
b
SDS extracts
0 30 0 30 0 30 E2 (min)
PAKT
AKT
HPIP
ERα
1 2 3 4 5 6
ShRNA Control
ShRNA MDM2 #1
ShRNA MDM2 #2
c
ShRNA Control
ShRNA MDM2 #1
ShRNA MDM2 #2
0 5 10 Tamoxifen (μM)
d
p53-depleted MCF7 cells
shRNA control
11.1%
23.7%
E2
p53-depleted MCF7 cells
shRNA MDM2#1
5.5%
9.2%
E2
Alexa Fluor 488
7-AAD
e
- E2
+ E2
GREB1
*
Fold induction
ShRNA
Control
MDM2
f
WT/WT Hypo/- Mouse genotype
HPIP
p53
TBK1
HSP90
1 2 3 4 5 6
g
WT/WT Hypo/- Mouse genotype
HPIP
p53
TBK1
α-tubulin
1 2 3 4 5 6
h
Lung
Heart
Spleen
Skeletal muscle
Prostate
Testis
Fat pad
WT/WT Hypo/- WT/WT Hypo/- WT/WT Hypo/- WT/WT Hypo/- WT/WT Hypo/- WT/WT Hypo/- WT/WT Hypo/- Mouse genotype
HPIP
HSP90
1 2 3 4 5 6 7 8 9 10 11 12 13 14
i
WT/WT Hypo/- Mouse genotype
0 30 0 30 0 30 0 30 E2 (min)
HPIP
PAKT
AKT
TBK1
1 2 3 4 5 6 7 8

Figure 7 MDM2 limits AKT activation by estrogens in control, but not in p53-deficient cells, and promotes tamoxifen resistance. (**a** and **b**) MDM2 depletion in p53-deficient MCF7 cells impairs E2-mediated AKT activation and leads to elevated HPIP and ERα levels. p53-depleted MCF7 cells were infected with the indicated lentiviral constructs and subsequently left untreated or stimulated with E2 (10 nM) for the indicated periods of time. Cytoplasmic (A) or total (B) extracts from the resulting cells were subjected to WB analysis. (**c**) MDM2 depletion in p53-deficient breast cancer cells sensitizes to tamoxifen. p53-depleted MCF7 cells were infected with the indicated lentiviral constructs and subsequently left untreated or stimulated with the indicated concentrations of tamoxifen. Foci were visualized after coloration with Giemsa. (**d** and **e**) MDM2 deficiency in p53-depleted MCF7 cells impairs E2-mediated cell proliferation (D) and E2-mediated GREB1 expression (E). FACS analyses were conducted on untreated or E2-stimulated p53-depleted MCF7 cells infected with the indicated lentiviral constructs (see Materials and Methods for details) (D). Percentage of cells in the S phase in each experimental condition is indicated. Total RNAs from control or shMDM2 p53-deficient MCF7 cells were subjected to quantitative real-time PCR analysis to assess GREB1 mRNA levels. The abundance of GREB1 mRNA levels in unstimulated p53-deficient MCF7 cells was set to 1 and GREB1 mRNA levels in other experimental conditions were relative to that after normalization with GAPDH ($^*P<0.05$, Student's *t*-test). The figure shows the data from three independent experiments performed on two distinct infections (mean values + S.D.). (**f** and **g**) Elevated HPIP levels in the mammary gland (F) or in the fat pad (male tissues) (G) of Mdm2-deficient mice. Protein extracts from wild-type (WT/WT) or hypomorphic (Hypo/ −) Mdm2 mice were made and subjected to WB analysis using the indicated antibodies. Anti-p53 WB analysis was performed to monitor p53 protein stabilization as a result of Mdm2 deficiency. (**h**) Elevated HPIP as a result of Mdm2 deficiency in a variety of tissues. Protein extracts from the indicated tissues were isolated in control or in Mdm2 hypomorphic mice and subjected to anti-HPIP or -HSP90 (loading control) WBs. (**i**) Impaired Mdm2 levels results in elevated HPIP and E2-mediated ^{P}AKT levels in primary cells. Mouse mammary epithelial cells from WT or hypomorphic mice were isolated and left untreated or stimulated with E2 for 30 min. WBs were conducted on the resulting protein extracts

anti-cytokeratin immunofluorescence analysis. The isolated primary MECs were plated at a density of about 2.5×10^5 cells/cm^2 in six-well plates that had been coated with collagen I (Gibco-BRL, Grand Islands, NY, USA). Cells seeded for 2 days in the plating media (DMEM/F12 medium, 5 μg/ml insulin, 2 μg/ml hydrocortisone, 5 ng/ml EGF, 50 μg/ml gentamycin, 100 U penicillin/streptomycin and 5% FCS) and switched to the estrogen-free media (DMEM/F12 medium without phenol red with 5% DCC) for 48 h.

FACS analysis to assess cell proliferation. MCF7 or MEC cells were left untreated or stimulated with E2 as described here before and subsequently incubated with 10 μM EdU for 2 h or 8 h (MCF7 and MEC cells, respectively). Cells were fixed and labeled using the Click-iT EdU cell proliferation assay kit (Invitrogen). Percentage of cells in the S phase was based on the amount of EdU-FITC-positive cells. 7-AAD (Sigma) was used for DNA content.

Immunofluorescence. MCF7 cells were seeded on coverslips in six-well plates and then fixed with paraformaldehyde 4% and preimmobilized with Triton X100 0.3% for 10 min at room temperature. Cells were then incubated with primary antibodies (TBK1 and HPIP) for 2 h at room temperature followed by 45 min of incubation at room temperature with secondary goat anti-rabbit FITC or goat anti-mouse Alexa Fluor 568-conjugated antibodies (Dako, Glostrup, Denmark). Images were acquired with the confocal system of Leica SP5 inverted microscope (Leica Microsystems, Wetzlar, Germany). DAPI stainings were carried out to visualize nuclei.

Yeast two-hybrid analysis. DNA encoding the C-terminal part of TBK1 (amino acids 529–729) was cloned into the GAL4 DNA-binding vector pGBKT7 (Clontech, Palo Alto, CA, USA) and used as bait in a two-hybrid screen of a human HeLa cDNA library in *Saccharomyces cerevisiae* Y187, according to the Matchmaker Two-hybrid System II protocol (Clontech). Positive yeast clones were selected for their ability to grow in the absence of histidine, leucine and tryptophan. Colonies were subsequently tested for β-galactosidase activity and DNAs from positive clones were identified by sequencing.

***In silico* analysis, kinase assays and IPs.** Potential HPIP phosphoacceptor sites were searched by submitting the human HPIP primary amino-acid sequence to Phosphosite (www.phosphosite.org). Kinase assays in transfected cells were carried out as described.[27,42] IPs involving ectopically expressed or endogenous proteins were carried out as described.[40,43] For the detection of endogenous polyubiquitinated forms of HPIP (Figure 4h), MCF7 cells were pretreated with MG132. Unstimulated or E2-treated MCF7 cells were lysed in a denaturing lysis buffer (Tris HCl 50 mM pH 8.0 , NaCl 150 mM, NP40 1%, deoxycholate Na 0.5%, SDS 1%). Genomic DNA was sheared with a needle and syringe and lysates were diluted 10 times in an incubating buffer (Tris HCl 50 mM pH 8.0 , NaCl 150 mM, NP40 1% with protease inhibitors) and precleared with control agarose (#UM400) (LifeSensors, Malvern, PA, USA) for 2 h at 4 °C. Cell lysates were subsequently incubated overnight at 4 °C with tandem ubiquitin binding entities (TUBEs) agarose (TUBE2, #UM402) (LifeSensors). Beads were subsequently washed five times with the incubating buffer, and polyubiquitinated forms of HPIP were visualized through anti-HPIP western blots.

For the detection of endogenous polyubiquitinated forms of HPIP in control *versus* MDM2-expressing MCF7 cells (Figure 5e), MG132-pretreated cells were lysed in a non denaturing conditions (Tris HCl 50 mM pH 8.0 , NaCl 150 mM, NP40 1%, deoxycholate Na 0.5%) and incubated with control agarose or with TUBE 2 for 1 h at 4 °C. Beads were subsequently washed five times with the incubating buffer and polyubiquitinated forms of HPIP were visualized through anti-HPIP western blots.

Chromatin IP assays. ChIP assays were essentially performed as described previously[39] by using the anti-p53 antibody or an IgG antibody as negative control. Extracts from control or p53-deficient MCF7 cells were precleared by 1 h incubation with protein A Sepharose/Herring sperm DNA and subsequent IPs were performed by incubating cell extracts overnight at 4 °C with the relevant antibody followed by 1 h of incubation with protein A/Herring sperm DNA. Protein–DNA complexes were washed as per standard ChIP techniques. After elution, proteinase K treatment and reversal of crosslinks, DNA fragments were analyzed by real-time PCR with SYBR green detection. Input DNA was analyzed simultaneously and used for normalization purposes. Primers used to address p53 recruitment on the *HPIP* (also referred to as *PBXIP*) gene promoter are listed in the Supplementary Table 1. Putative p53-binding sites were identified by combining searches using algorithms developed in the p53FamTag website (sites F and J) and by Sabiosciences (http://www.sabiosciences.com/chipqpcrsearch.php?app=TFBS; sites A, B, C, D, E and G). p53 sites located at $\sim$3500 bp upstream the TSS (Figure 6c, sites E and F) were identified in both databases.

Lentiviral infections and real-time PCRs. ShRNA control, MDM2, TBK1 and HPIP lentiviral constructs were all from Sigma. Lentiviral infections of control, p53-deficient MCF7 or MDA-MB-231 cells with shRNA constructs were carried out as previously described, as were real-time PCR analysis.[43] Sequences of primers used to assess GREB1, p21 and HPIP are available on request.

Screening of the siRNA E3 ligase library. A human E3 ligase library (G-005600, Dharmacon, Lafayette, CO, USA) was screened according to the protocol provided by the manufacturer. Briefly, MCF7 cells were transfected in 96 wells with a pool of distinct siRNAs targeting the same transcripts in duplicate using HiPerfect reagent (Qiagen). After 48 h of transfection, cells were harvested, lysed with 1% SDS buffer and HPIP, TBK1 and α-tubulin protein levels were assessed by western blot analysis. All signals were quantified by densitometry. The HPIP/α-tubulin ratio obtained in MCF7 transfected with the GFP siRNA was set to 1, and the ratio obtained in other experimental conditions was expressed relative to that. Any candidate whose siRNA-mediated depletion gave a HPIP/α-tubulin ratio similar or higher to the one obtained in TBK1-depleted cells (positive control) was selected. A second screening performed with the selected siRNA sequences was subsequently carried out for confirmatory purposes. Data from the second screening are shown.

Conflict of Interest

The authors declare no conflict of interest.

Acknowledgements. We are grateful to E Dejardin for helpful discussions and to the GIGA Imaging and Flow Cytometry Platform for performing the FACS and IF analyses. This work was supported by grants from the FNRS, TELEVIE, the Belgian Federation against cancer, the King Baudouin Fundation, the University of Liege (Concerted Research Action Program (BIO-ACET) and 'Fonds Spéciaux', the Inter-University Attraction Pole 6/12 (Federal Ministery of Science), the 'Plan Cancer (Action 29)', the 'Centre Anti-Cancéreux' and the 'Leon Fredericq' Fundation (ULg) as well as by the Walloon Excellence in Life Sciences and Biotechnology (WELBIO). PC, LN and AC are Research Associates and Senior Research Associate at the Belgian National Funds for Scientific Research (FNRS), respectively.

1. Mandinova A, Lee SW. The p53 pathway as a target in cancer therapeutics: obstacles and promise. *Sci Transl Med* 2011; **3**: 64rv61.
2. Vu BT, Vassilev L. Small-molecule inhibitors of the p53-MDM2 interaction. *Curr Top Microbiol Immunol* 2011; **348**: 151–172.
3. Marine JC, Lozano G. Mdm2-mediated ubiquitylation: p53 and beyond. *Cell Death Differ* 2010; **17**: 93–102.
4. Yang JY, Zong CS, Xia W, Yamaguchi H, Ding Q, Xie X *et al.* ERK promotes tumorigenesis by inhibiting FOXO3a via MDM2-mediated degradation. *Nat Cell Biol* 2008; **10**: 138–148.
5. Kurokawa M, Kim J, Geradts J, Matsuura K, Liu L, Ran X *et al.* A Network of substrates of the E3 ubiquitin ligases MDM2 and HUWE1 control apoptosis independently of p53. *Sci Signal* 2013; **6**: ra32.
6. Hers I, Vincent EE, Tavare JM. Akt signalling in health and disease. *Cell Signal* 2011; **23**: 1515–1527.
7. Manning BD, Cantley LC. AKT/PKB signaling: navigating downstream. *Cell* 2007; **129**: 1261–1274.
8. Yuan TL, Cantley LC. PI3K pathway alterations in cancer: variations on a theme. *Oncogene* 2008; **27**: 5497–5510.
9. Altomare DA, Testa JR. Perturbations of the AKT signaling pathway in human cancer. *Oncogene* 2005; **24**: 7455–7464.
10. Manavathi B, Acconcia F, Rayala SK, Kumar R. An inherent role of microtubule network in the action of nuclear receptor. *Proc Natl Acad Sci USA* 2006; **103**: 15981–15986.
11. Abramovich C, Shen WF, Pineault N, Imren S, Montpetit B, Largman C *et al.* Functional cloning and characterization of a novel nonhomeodomain protein that inhibits the binding of PBX1-HOX complexes to DNA. *J Biol Chem* 2000; **275**: 26172–26177.
12. Manavathi B, Lo D, Bugide S, Dey O, Imren S, Weiss MJ *et al.* Functional regulation of pre-B-cell leukemia homeobox interacting protein 1 (PBXIP1/HPIP) in erythroid differentiation. *J Biol Chem* 2012; **287**: 5600–5614.
13. Andjelkovic M, Jakubowicz T, Cron P, Ming XF, Han JW, Hemmings BA. Activation and phosphorylation of a pleckstrin homology domain containing protein kinase (RAC-PK/PKB) promoted by serum and protein phosphatase inhibitors. *Proc Natl Acad Sci USA* 1996; **93**: 5699–5704.
14. Gao T, Furnari F, Newton AC. PHLPP: a phosphatase that directly dephosphorylates Akt, promotes apoptosis, and suppresses tumor growth. *Mol Cell* 2005; **18**: 13–24.
15. Trotman LC, Alimonti A, Scaglioni PP, Koutcher JA, Cordon-Cardo C, Pandolfi PP. Identification of a tumour suppressor network opposing nuclear Akt function. *Nature* 2006; **441**: 523–527.
16. Ugi S, Imamura T, Maegawa H, Egawa K, Yoshizaki T, Shi K *et al.* Protein phosphatase 2A negatively regulates insulin's metabolic signaling pathway by inhibiting Akt (protein kinase B) activity in 3T3-L1 adipocytes. *Mol Cell Biol* 2004; **24**: 8778–8789.
17. Song MS, Salmena L, Pandolfi PP. The functions and regulation of the PTEN tumour suppressor. *Nat Rev Mol Cell Biol* 2012; **13**: 283–296.
18. Suizu F, Hiramuki Y, Okumura F, Matsuda M, Okumura AJ, Hirata N *et al.* The E3 ligase TTC3 facilitates ubiquitination and degradation of phosphorylated Akt. *Dev Cell* 2009; **17**: 800–810.
19. Bae S, Kim SY, Jung JH, Yoon Y, Cha HJ, Lee H *et al.* Akt is negatively regulated by the MULAN E3 ligase. *Cell Res* 2012; **22**: 873–885.
20. Barbie DA, Tamayo P, Boehm JS, Kim SY, Moody SE, Dunn IF *et al.* Systematic RNA interference reveals that oncogenic KRAS-driven cancers require TBK1. *Nature* 2009; **462**: 108–112.
21. Korherr C, Gille H, Schafer R, Koenig-Hoffmann K, Dixelius J, Egland KA *et al.* Identification of proangiogenic genes and pathways by high-throughput functional genomics: TBK1 and the IRF3 pathway. *Proc Natl Acad Sci USA* 2006; **103**: 4240–4245.
22. Shen RR, Hahn WC. Emerging roles for the non-canonical IKKs in cancer. *Oncogene* 2011; **30**: 631–641.
23. Burris HA 3rd. Overcoming acquired resistance to anticancer therapy: focus on the PI3K/AKT/mTOR pathway. *Cancer Chemother Pharmacol* 2013; **71**: 829–842.
24. Ou YH, Torres M, Ram R, Formstecher E, Roland C, Cheng T *et al.* TBK1 directly engages Akt/PKB survival signaling to support oncogenic transformation. *Mol Cell* 2011; **41**: 458–470.
25. Xie X, Zhang D, Zhao B, Lu MK, You M, Condorelli G *et al.* IkappaB kinase epsilon and TANK-binding kinase 1 activate AKT by direct phosphorylation. *Proc Natl Acad Sci USA* 2011; **108**: 6474–6479.
26. Guo JP, Coppola D, Cheng JQ. IKBKE protein activates Akt independent of phosphatidylinositol 3-kinase/PDK1/mTORC2 and the pleckstrin homology domain to sustain malignant transformation. *J Biol Chem* 2011; **286**: 37389–37398.
27. Gatot JS, Gioia R, Chau TL, Patrascu F, Warnier M, Close P *et al.* Lipopolysaccharide-mediated interferon regulatory factor activation involves TBK1-IKKepsilon-dependent Lys(63)-linked polyubiquitination and phosphorylation of TANK/I-TRAF. *J Biol Chem* 2007; **282**: 31131–31146.
28. Fujita F, Taniguchi Y, Kato T, Narita Y, Furuya A, Ogawa T *et al.* Identification of NAP1, a regulatory subunit of I kappa B kinase-related kinases that potentiates NF-kappa B signaling. *Mol Cell Biol* 2003; **23**: 7780–7793.
29. Pomerantz JL, Baltimore D. NF-kappa B activation by a signaling complex containing TRAF2, TANK and TBK1, a novel IKK-related kinase. *Embo J* 1999; **18**: 6694–6704.
30. Yamaoka S, Courtois G, Bessia C, Whiteside ST, Weil R, Agou F *et al.* Complementation cloning of NEMO, a component of the IkappaB kinase complex essential for NF-kappaB activation. *Cell* 1998; **93**: 1231–1240.
31. Rae JM, Johnson MD, Scheys JO, Cordero KE, Larios JM, Lippman ME. GREB 1 is a critical regulator of hormone dependent breast cancer growth. *Breast Cancer Res Treat* 2005; **92**: 141–149.
32. Campbell RA, Bhat-Nakshatri P, Patel NM, Constantinidou D, Ali S, Nakshatri H. Phosphatidylinositol 3-kinase/AKT-mediated activation of estrogen receptor alpha: a new model for anti-estrogen resistance. *J Biol Chem* 2001; **276**: 9817–9824.
33. Keutgens A, Shostak K, Close P, Zhang X, Hennuy B, Aussems M *et al.* The Repressing Function of the Oncoprotein BCL-3 Requires CtBP, while Its Polyubiquitination and Degradation Involve the E3 Ligase TBLR1. *Mol Cell Biol* 2010; **30**: 4006–4021.
34. Duong V, Boulle N, Daujat S, Chauvet J, Bonnet S, Neel H *et al.* Differential regulation of estrogen receptor alpha turnover and transactivation by Mdm2 and stress-inducing agents. *Cancer Res* 2007; **67**: 5513–5521.
35. Vassilev LT, Vu BT, Graves B, Carvajal D, Podlaski F, Filipovic Z *et al.* In vivo activation of the p53 pathway by small-molecule antagonists of MDM2. *Science* 2004; **303**: 844–848.
36. Patel S, Player MR. Small-molecule inhibitors of the p53-HDM2 interaction for the treatment of cancer. *Expert Opin Invest Drugs* 2008; **17**: 1865–1882.
37. Mendrysa SM, McElwee MK, Michalowski J, O'Leary KA, Young KM, Perry ME. mdm2 Is critical for inhibition of p53 during lymphopoiesis and the response to ionizing irradiation. *Mol Cell Biol* 2003; **23**: 462–472.
38. Callige M, Richard-Foy H. Ligand-induced estrogen receptor alpha degradation by the proteasome: new actors? *Nucl Recept signal* 2006; **4**: e004.
39. Close P, Hawkes N, Cornez I, Creppe C, Lambert CA, Rogister B *et al.* Transcription impairment and cell migration defects in elongator-depleted cells: implication for familial dysautonomia. *Mol cell* 2006; **22**: 521–531.
40. Viatour P, Dejardin E, Warnier M, Lair F, Claudio E, Bureau F *et al.* GSK3-mediated BCL-3 phosphorylation modulates its degradation and its oncogenicity. *Mol cell* 2004; **16**: 35–45.
41. Chariot A, Leonardi A, Muller J, Bonif M, Brown K, Siebenlist U. Association of the adaptor TANK with the I kappa B kinase (IKK) regulator NEMO connects IKK complexes with IKK epsilon and TBK1 kinases. *J Biol Chem* 2002; **277**: 37029–37036.
42. Leonardi A, Chariot A, Claudio E, Cunningham K, Siebenlist U. CIKS, a connection to Ikappa B kinase and stress-activated protein kinase. *Proc Natl Acad Sci USA* 2000; **97**: 10494–10499.
43. Robert I, Aussems M, Keutgens A, Zhang X, Hennuy B, Viatour P *et al.* Matrix Metalloproteinase-9 gene induction by a truncated oncogenic NF-kappaB2 protein involves the recruitment of MLL1 and MLL2 H3K4 histone methyltransferase complexes. *Oncogene* 2009; **28**: 1626–1638.
44. Keutgens A, Zhang X, Shostak K, Robert I, Olivier S, Vanderplasschen A *et al.* BCL-3 degradation involves its polyubiquitination through a FBW7-independent pathway and its binding to the proteasome subunit PSMB1. *J Biol Chem* 2010; **285**: 25831–25840.

Supplementary Information accompanies this paper on Cell Death and Differentiation website (http://www.nature.com/cdd)